

EVALUATION OF EMITTER LOCATION ACCURACY WITH THE MODIFIED TRIANGULATION METHOD BY MEANS OF MAXIMUM LIKELIHOOD ESTIMATORS

Jan Matuszewski, Tomasz Kraszewski

*Military University of Technology, Faculty of Electronics, Institute of Radioelectronics, gen. S. Kaliskiego 2,
 00-908 Warsaw, Poland* (✉ jan.matuszewski@wat.edu.pl, +48 261 837 571, tomasz.kraszewski@wat.edu.pl)

Abstract

The determination of precise emitter location is a very important task in electronic intelligence systems. Its basic requirements include the detection of the emission of electromagnetic sources (emitters), measurement of signal parameters, determining the direction of emitters, signal analysis, and the recognition and identification of their sources. The article presents a new approach and algorithm for calculating the location of electromagnetic emission sources (radars) in a plane based on the bearings in the radio-electronic reconnaissance system. The main assumptions of this method are presented and described *i.e.* how the final mathematical formulas for calculating the emitter location were determined for any number of direction finders (DFs). As there is an unknown distance from the emitter to the DFs then in the final formulas it is stated how this distance should be calculated in the first iteration. Numerical simulation in MATLAB showed a quick convergence of the proposed algorithm to the fixed value in the fourth/fifth iteration with an accuracy less than 0.1 meter. The computed emitter location converges to the fixed value regardless of the choice of the starting point. It has also been shown that to precisely calculate the emitter position, at least a dozen or so bearings from each DFs should be measured. The obtained simulation results show that the precise emitter location depends on the number of DFs, the distances between the localized emitter and DFs, their mutual deployment, and bearing errors. The research results presented in the article show the usefulness of the tested method for the location of objects in a specific area of interest. The results of simulation calculations can be directly used in radio-electronic reconnaissance systems to select the place of DFs deployment to reduce the emitter location errors in the entire reconnaissance area.

Keywords: emitter location, triangulation method, errors ellipse, maximum likelihood estimators, electronic warfare.

© 2021 Polish Academy of Sciences. All rights reserved

1. Introduction

Electronic Intelligence (ELINT) and *Electronic Support Measures* (ESM) systems perform the functions of threat detection and area surveillance to determine the identity and bearing of surrounding electromagnetic emissions from airborne, seaborne, and ground-based platforms.

Copyright © 2021. The Author(s). This is an open-access article distributed under the terms of the Creative Commons Attribution-NonCommercial-NoDerivatives License (CC BY-NC-ND 4.0 <https://creativecommons.org/licenses/by-nc-nd/4.0/>), which permits use, distribution, and reproduction in any medium, provided that the article is properly cited, the use is non-commercial, and no modifications or adaptations are made.

Article history: received March 24, 2021; revised July 20, 2021; accepted August 24, 2021; available online August 31, 2021.

These systems are entirely passive in that they do not emit electromagnetic emissions and are used for measuring the direction of incoming target threat emissions. The emitter's coordinates can be estimated by a single moving observation system via its receiver, which measures the signal parameters from the emitter, or by using multiple *direction finders* (DFs). ELINT and ESM systems incorporate a passive receiver to measure the parameters of the received signals and an automatic processor to identify and classify the incoming emitter's signals [1–4].

These signal parameters, which correspond to geometric quantities, are the direction/*angle of arrival* (AOA) obtained from the measured amplitude or range difference from the emitter to the two measurement points obtainable from the *time difference of arrival* (TDOA). The actual location technique depends upon the kind of signal parameters being measured, the measurement techniques, and the data processing procedures [3, 5–13].

Conventional ESM systems measure the basic parameters of incoming emitter signals (frequency, amplitude, bearing angle, pulse width, *time of arrival* (TOA)). The collected data are sorted into groups considered to be from a single emitter and used to compute the time-dependent parameters (pulse repetition frequency, antenna rotating period, type of modulation, etc.) [14].

Another possible method is to measure the time difference of arrival of the emitter signal at several dispersed sensors which are located substantially further away than the wavelength. With multiple platforms, measurements of an emitter's time of arrival from one sensor can be used with TOA measurements from another to compute a time difference of arrival. Each TDOA forms a hyperbola on the plane. Each hyperbola represents a specific TDOA and is called an isochrone [15–18]. An intersection of TDOA isochrones provides the estimates of emitter location. If the time difference of arrival is measured very accurately, the emitter location will be very close to this intersection of isochrones.

The method of emitter location based on the bearings received from two or more spatially deployed DFs is commonly called the triangulation method. Because of the uncertainties in the angle of arrival measurements, uncertainties exist in the estimated emitter location. The emitter's location is a significant parameter in the overall process of determining its possible application [15, 16, 19].

The errors of emitter location depend both on the measurement accuracy of the DFs and their deployment in the electromagnetic environment. In order to calculate the emitter's location, the ESM system requires information from a minimum of two DFs, which are deployed at a specific distance from each other, called the system baseline [20–22]. The coordinates of the emitter's location (position) were determined with an error, which is generally a function of all errors occurring in the emitter location system and introduced by the system's environment [23–26]. In a real electromagnetic environment, the most important errors are those associated with the accuracy of the bearing measurements in the DFs.

The emitter location estimation algorithm is based on the classical observation model and the maximum likelihood estimators in the case of assuming the known measured bearing errors for all DFs [2, 27]. This algorithm can be generalized to make use of bearing measurements which have different accuracies and which can be taken at different ranges.

A correctly determined emitter location and its identification allow for the provision of important information for military command systems, and for managing active means of jamming in *Electronic Warfare* (EW) systems [2, 28, 29]. The analysis of the real possibility of increasing the accuracy of emitter location was carried out on the example of ESM stations used in practice, and which constitute the basic elements of a tactical location system. The method of emitter location based on AOA measurements is one of the most popular location methods and at the same time one of the easiest to implement. The location of the electromagnetic sources in the triangulation method is geometrically determined based on the bearings obtained from individual DFs.

The proposed algorithm for estimating the emitter's location is based on the assumption of the known Gaussian distribution of measured bearing errors. The accuracy of determining the location of the emission's source can be described through various characteristics, amongst which a common feature is a fact that the accuracy is described on the plane by an elliptical or a circular error [30–32]. These errors should cover this calculated emitter location with a definite probability [14, 15, 33–35].

In the reconnaissance and electronic warfare systems, the time of identifying the emitters and determining their position is very important. In the triangulation method, the calculated position of the emitter based on single bearings to the emission source can be burdened with a large error. In addition, the probability of detecting the signal depends on the speed of rotation of the antennas and the width of their characteristics. As a rule, it takes a few turns of the antennas to be able to accurately measure the bearing to the emission source, then at the leading station, it is necessary to associate these bearings obtained from the beacons and then calculate the position of the emitter on their basis. The algorithm presented in the paper, the computing program developed in MATLAB®, and the conclusions from simulation tests can be directly used in a real radio-electronic reconnaissance system to accelerate the process of identifying and locating the sources of emission. It is also very important to compare the localization errors for the same emitter position test points. Conclusions from the simulation calculations can be useful for the operator in the reconnaissance station to accelerate the process of measuring the parameters of radar signals and initially rejecting bearings with a large error. The simulation tests of the properties of the method described in the article can also be useful for selecting the position of the bearings because the actual measurement errors of the bearings and the possible size of the monitored area were used in these calculations.

Our new approach to the triangulation method contains:

- derivation of mathematical formulas for calculation of the emitter position in the absence of a priori information about its position using the greatest reliability method for any number of *direction finders* (DFs);
- development of an algorithm for the modified triangulation method and computing program;
- explanation how to calculate an unknown distance from DFs to unknown emitter location in the first step of iteration;
- validation convergence of calculated emitter's position to its tested location for the proposed algorithm;
- comparison of different emitter location errors on the basis of simulation experiments for the same scenarios of the DFs and emitter deployment.

The rest of the paper is organized as follows: in Section 2, the background and the main idea of the triangulation method of emitter location are introduced. In Section 3, the problem to be solved is formally defined and the appropriate algorithm is presented. Section 4 mainly contains experimental details and results, as well as comprehensive analyses. The accuracy of emitter location is measured in terms of the standard deviation compared to the actual emitter's position and was tested using simulated data in the MATLAB environment. Section 5 provides the conclusion of the entire paper.

2. A description of the triangulation method

The AOA of a signal, or its line of bearing, is a parameter frequently used for calculating an emitter's location. If the emitter is located on a plane, then measurement of only two bearings θ_1 and θ_2 from two sensors (DF₁ and DF₂) deployed at a given distance d in the points A and B is

sufficient to determine its location. The evaluation of emitter location (point E) is determined by the point of intersection of two bearing lines, which are here the position lines as shown in Fig. 1.

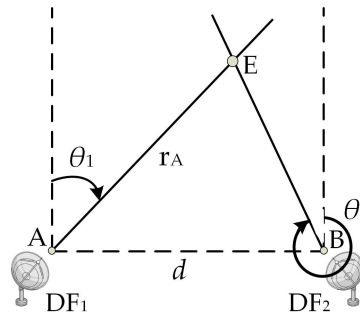


Fig. 1. Triangulation method for emitter location based on two bearings.

Due to occurring angle errors, the bearings seldom intersect in one single point. In the case of three DF sensors, the line of bearings forms a triangle of error. Therefore, a need arises to assign the most probable point P in which the emitter is placed (Fig. 2a). The task becomes even more complicated when more than three DFs are used (Fig. 2b). The triangulation method can be implemented on all varieties of platforms, including aircraft, ships, and ground vehicles.

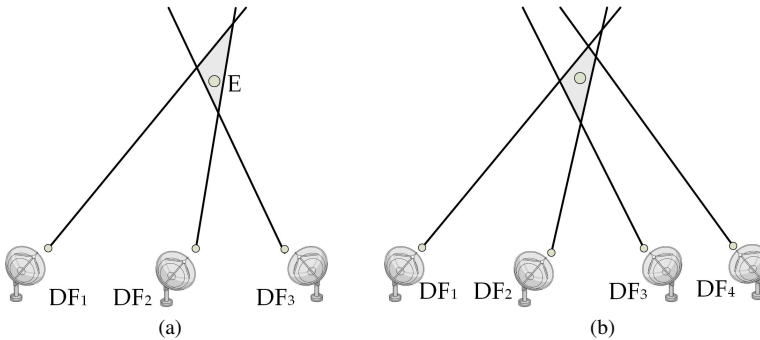


Fig. 2. Triangulation method for emitter location based on (a) a triangle area of errors, and (b) a quadrilateral error area.

The distance r_A from point A to the emitter (E) in Fig. 1 is calculated from the formula

$$r_A = \frac{d}{\sin \theta_1 - \cos \theta_1 \tan \theta_2}. \quad (1)$$

Since each bearing is affected by a measurement error, the calculated emitter location based on many different bearings creates a specific area on the plane called the region of uncertainty, in which the detected emitter is located with a certain probability. To determine the coordinates of the emitter, a certain minimum number of bearing measurements made on the same electromagnetic source is required. The accuracy of determining the position of the emission source is assessed here on the basis of a statistical analysis of the measurement results.

In practice, the calculated location of the emitter is not a point but a kite-shaped, circular or elliptical area, as shown in Fig. 3. The estimation of emitter location in the conditions of having no a priori information using the maximum likelihood method is presented in the next section.

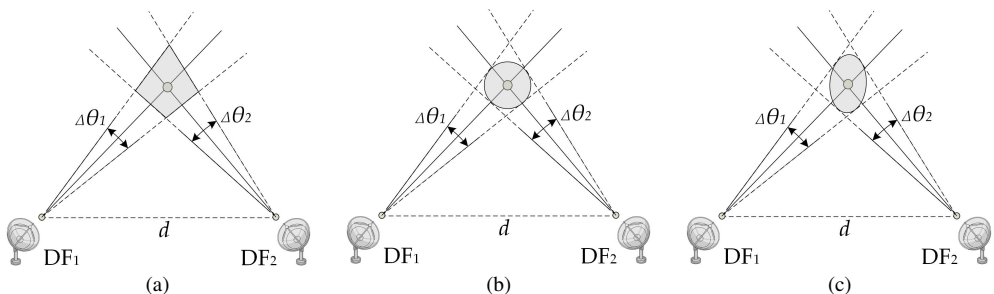


Fig. 3. Area of errors in the triangulation method of emitter location for two direction finders: (a) A kite-shaped error area, (b) a circular error area, and (c) an elliptical error area.

3. Basic mathematical dependencies concerning the calculations of emitter location

Due to bearing measurement errors, the emitter location is not indicated as a precise point but only as an area in which the detected object is placed with a given probability. Assuming that the DFs and emitter are deployed on the plane OXY , the location of the i -th DF will be marked as a function of coordinates $r_i = f_i(x_i, y_i)$ and the real emitter location (E) by a function $r = f(x, y)$ (Fig. 4).

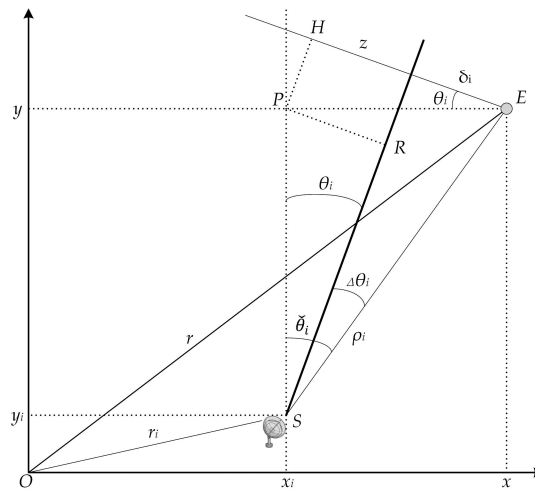


Fig. 4. Area of errors in the triangulation method of emitter location for two direction finders.

In every point of signal receiving (x_i, y_i) the bearings θ_i are measured. In an electromagnetic environment, every real bearing θ_i is measured with a measurement error $\Delta\theta_i$, that is:

$$\Delta\theta_i = \check{\theta}_i - \theta_i, \quad i = 1, 2, \dots, n \quad (2)$$

or

$$\theta_i = \check{\theta}_i \pm |\Delta\theta_i|, \quad (3)$$

where $\check{\theta}_i$ is the ideal bearing (errorless), $|\Delta\theta_i|$ is the value of absolute error $\Delta\theta_i$, and n is the number of DFs.

Based on Fig. 4, the angle $\check{\theta}_i$ can be calculated from the following relation:

$$\check{\theta}_i = \arctan \frac{x - x_i}{y - y_i} = f(x, y, x_i, y_i) = f_i(x, y). \quad (4)$$

It is assumed that these errors $\Delta\theta_i$ are independent and have a normal distribution, with the mean value equalling zero and with standard deviation ξ_i . In the emitter location estimation, using a method of the greatest reliability, such coordinates (x^*, y^*) are searched for which the Gaussian density function of bearings $(\theta_1, \theta_2, \dots, \theta_n)$ reaches the maximum on the condition that this detected emitter is situated in the point (x, y) [21, 29, 33].

The estimation of emitter location in the conditions of a lack of a priori information can be carried out using a method of the greatest reliability. This function can be described using the following formula [9, 36]:

$$L(\theta_1, \theta_2, \dots, \theta_n; x, y) = p(\theta_1, \theta_2, \dots, \theta_n/x, y) = \prod_{i=1}^n \frac{1}{\sqrt{2\pi}\sigma_i} \exp \left\{ -\frac{[\Delta\theta_i(x, y)]^2}{2\sigma_i^2} \right\}. \quad (5)$$

The bearing error for the i -th DF will now be determined in the function of coordinates (x, y) . Assuming that this error is small, the following formula can be written as

$$\Delta\theta_i(x, y) = \frac{\delta_i(x, y)}{\rho_i}, \quad (6)$$

where ρ_i denotes the approximately defined unknown distance from the i -th DF to the emitter, as follows:

$$\rho_i = \sqrt{(x_0 - x_i)^2 + (y_0 - y_i)^2}. \quad (7)$$

In this formula, values x_0, y_0 denote the approximately defined initial coordinates of real emitter location. Using the trigonometric relation in the EHP and PRS triangles (Fig. 4), we obtain:

$$\delta_i(x, y) = (x - x_i) - z, \quad (8)$$

$$z = (y - y_i) \sin \theta_i. \quad (9)$$

Setting (9) to (8), we obtain:

$$\delta_i(x, y) = (x - x_i) \cos \theta_i - (y - y_i) \sin \theta_i. \quad (10)$$

Next, assuming that:

$$p(\theta_1, \theta_2, \dots, \theta_n/x, y) = K \cdot \exp \left[-\frac{1}{2} \sum_{i=1}^n \frac{\delta_i^2(x, y)}{\sigma_i^2 \rho_i^2} \right], \quad (11)$$

where

$$K = \left[(2\pi)^{n/2} \prod_{i=1}^n \sigma_i \right]^{-1} \quad (12)$$

then the likelihood function can be represented as:

$$L(\theta_1, \theta_2, \dots, \theta_n; x, y) = p(\theta_1, \theta_2, \dots, \theta_n/x, y) = K \cdot \exp \left[-\frac{1}{2} \lambda(x, y) \right]. \quad (13)$$

The $\lambda(x, y)$ function in (13) denotes the uncertainty function expressed by the formula:

$$\lambda(x, y) = Ax^2 + 2Bxy + Cy^2 + 2Dx + 2Ey + F, \quad (14)$$

where the respective coefficients are calculated from the following formulae:

$$A = \sum_{i=1}^n \frac{\cos^2 \theta_i}{\sigma_i^2 \rho_i^2}, \quad B = -\frac{1}{2} \sum_{i=1}^n \frac{\sin(2\theta_i)}{\sigma_i^2 \rho_i^2}, \quad (15)$$

$$C = \sum_{i=1}^n \frac{\sin^2 \theta_i}{\sigma_i^2 \rho_i^2}, \quad D = -\sum_{i=1}^n \frac{x_i \cos^2 \theta_i - 0.5y_i \sin(2\theta_i)}{\sigma_i^2 \rho_i^2}, \quad (16)$$

$$E = \sum_{i=1}^n \frac{0.5x_i \sin(2\theta_i) - y_i \sin^2 \theta_i}{\sigma_i^2 \rho_i^2}, \quad F = \sum_{i=1}^n \frac{(x_i \cos \theta_i - y_i \sin \theta_i)^2}{\sigma_i^2 \rho_i^2}. \quad (17)$$

The optimal estimators (x^*, y^*) from the point of view of maximum likelihood fulfil here the condition of the maximization of the function $L(\theta_1, \theta_2, \dots, \theta_n; x, y)$, which is equivalent to the task of the minimization of the following function $\lambda(x, y)$, which can be written as:

$$\lambda L(\theta_1, \theta_2, \dots, \theta_n; x^*, y^*) = \max \iff (x^*, y^*) = \min. \quad (18)$$

The minimum of the function $\lambda(x, y)$ defined by formula (14) is calculated from the following set of equations:

$$\left. \frac{\partial \lambda}{\partial x} \right|_{x=x^*} = 2(Ax^* + By^* + D) = 0, \quad (19)$$

$$\left. \frac{\partial \lambda}{\partial y} \right|_{y=y^*} = 2(Bx^* + Cy^* + E) = 0. \quad (20)$$

After solving the set of equations (19)–(20), the final formulae for optimal estimators (x^*, y^*) of the emitter location coordinates have the following form:

$$x^* = \frac{BE - CD}{AC - B^2}, \quad y^* = \frac{BD - AE}{AC - B^2}. \quad (21)$$

From (21), the condition that $AC - B^2 > 0$ arises. Because (15)–(17) are in the entangled form (on the right side are unknown values in the expression at ρ_i), the initial values ρ_i are calculated approximately and then improved in the next iterations by the method of successive approximation. For the approximation, the initial value ρ_i is taken as the distance from the i -th DF site to the point of intersection with the bearing θ_i from the i -th DF with any line of angle θ_j from the j -th DF site.

The accuracy of determining emitter location can be described by various characteristics. A common feature of these characteristics is that the accuracy on the plane is described by an area in the form of the so-called error ellipse with a given probability P_e . This ellipse covers the emitter location or an area in the form of the so-called circle of errors with a given probability P_k of covering this place with this circle. The error ellipse most precisely defines the accuracy of emitter location on the plane for the set values of ρ_i and θ_i . The properties of the error ellipse are characterized by the maximum probability of covering the emitter's location among all possible geometric figures with the same surface area.

The disadvantage of this description, however, is the necessity to calculate (for a fixed P_e) three parameters: two main axes and the angle of inclination of the error ellipse, defining the

direction of the semi-major axis in relation to the selected axis of the coordinate system as the reference direction. In the case of many different positions of the emitter, *i.e.*, the corresponding different values of ρ_i and θ_i , the accuracy of determining the position of the emitter is determined by the set of ellipses, forming the so-called error area.

Taking into account the rotation of the OXY coordinate system by angle α clockwise, all the bearings θ_i in the new OUV coordinate system will take the following values: $\theta_i - \alpha$, *i.e.*:

$$A_1 = \sum_{i=1}^n \frac{\cos^2(\theta_i - \alpha)}{\sigma_i^2 \rho_i^2}, \quad B_1 = -\frac{1}{2} \sum_{i=1}^n \frac{\sin 2(\theta_i - \alpha)}{\sigma_i^2 \rho_i^2}, \quad C_1 = \sum_{i=1}^n \frac{\sin^2(\theta_i - \alpha)}{\sigma_i^2 \rho_i^2}. \quad (22)$$

From (22), we get the following relation:

$$\tan(2\alpha) = \frac{\sum_{i=1}^n \frac{\sin(2\theta_i)}{\rho_i^2 \sigma_i^2}}{\sum_{i=1}^n \frac{\cos(2\theta_i)}{\rho_i^2 \sigma_i^2}}, \quad (23)$$

from which we calculate the orientation angle α of the error ellipse, counting clockwise to the reference direction, *i.e.*, the northern direction. Angle α indicates the slope of the error ellipse with respect to the Oy axis [26, 31].

Standard deviations σ_u and σ_v of the ellipse of errors in the orthogonal directions, *i.e.*, the maximum and minimum mean square error, respectively, can be determined from the following relation:

$$\sigma_u = A_1^{-\frac{1}{2}}, \quad \sigma_v = C_1^{-\frac{1}{2}}, \quad (24)$$

from where

$$\sigma_x = \sigma_u \sin \alpha, \quad \sigma_y = \sigma_v \cos \alpha. \quad (25)$$

The two-dimensional posterior normal distribution in the new coordinate system has the form:

$$p(u, v/\theta_1, \theta_2, \dots, \theta_n) = \frac{1}{2\pi\sigma_u\sigma_v} \exp \left[-\frac{1}{2} \left(\frac{u^2}{\sigma_u^2} + \frac{v^2}{\sigma_v^2} \right) \right]. \quad (26)$$

As a result of the cross-section of the surface of this distribution with the $p = const$ planes and the projection of the obtained contours onto the OUV plane, we obtain a family of ellipses of errors, described by the equation:

$$\frac{u^2}{\sigma_u^2} + \frac{v^2}{\sigma_v^2} = k^2, \quad (27)$$

where k is the error ellipse parameter.

Hence the axes of the error ellipse are expressed by the following dependencies:

$$a = k\sigma_u, \quad b = k\sigma_v \quad (28)$$

while the area of the ellipse of errors is calculated from the following equation:

$$S_e = \pi ab = \pi k^2 \sigma_u \sigma_v. \quad (29)$$

The value of parameter $k = k_0$ for a given probability ($k_0 = P_0$) of the occurrence of the emitter in the ellipse of errors (or the coverage of the emitter with an ellipse) can be determined from the formula:

$$k_0 = \sqrt{-2 \ln(1 - P_0)}. \quad (30)$$

For $k_0 = 1$, i.e., for the so-called unit error ellipse (where $a = k\sigma_x$, $b = k\sigma_y$) the value $P_k = 0.393$.

In addition, except for the area errors, the numerical values of the parameters can also be used to evaluate the accuracy of the system's location. The most commonly used for this purpose are the circular error, geometric error, and mean square error.

In order to assess the accuracy of the location of electromagnetic sources, we can use the circular error probability (*CEP*), calculated according to the following relation:

$$CEP = \sqrt{\sigma_x^2 + \sigma_y^2} \sqrt{\left(1 - \frac{2/\left(\sigma_x^2 + \sigma_y^2\right)^2 (\sigma_x^4 + \sigma_y^4)}{9}\right)^3} \quad (31)$$

and the geometric mean error (*GME*):

$$GME = 1.177 \sqrt{\sigma_x \sigma_y}. \quad (32)$$

The *CEP* error is defined as the radius of the circle centred on the calculated emitter location that provides a 50% probability that the actual emitter location is within the circle [1, 13]. The *GME* error is defined as a radius with an area equal to the probable area of error ellipse ($P_k = 0.5$). The *GME* error has the property that if any of the standard deviations σ_x , σ_y is equal to zero, this measure will also be equal to zero, although the second deviation value may be very large.

Based on N observations (the bearings taken from each DF to the emitter), the average position of the emitter is calculated as follows:

$$\bar{x} = \frac{1}{N} \sum_{i=1}^N x_i^*, \quad \bar{y} = \frac{1}{N} \sum_{i=1}^N y_i^*, \quad (33)$$

where the estimators x_i^* , y_i^* of the emitter's position are determined using formulas (21).

The mean square errors σ_x , σ_y in determining the emitter's location for the x and y coordinates respectively are calculated from the following formulas:

$$\sigma_x = \sqrt{\frac{1}{N} \sum_{i=1}^N (x_i^* - \bar{x})^2}, \quad \sigma_y = \sqrt{\frac{1}{N} \sum_{i=1}^N (y_i^* - \bar{y})^2} \quad (34)$$

and the mean linear error:

$$\sigma = \sqrt{\sigma_x^2 + \sigma_y^2}. \quad (35)$$

The algorithm presented in Fig. 5 can use two different rules for stopping the calculation of the emitter location process:

- a) according to the assumed permissible number of k_{\max} of consecutive approximations of value (x^*, y^*) ;
- b) according to the assumed acceptable value changes $(\Delta x_{\max}, \Delta y_{\max})$ of the coordinates of the emitter's location subject to successive approximations.

In the first rule, the iteration process is stopped when the condition $k \geq k_{\max}$ is satisfied. The disadvantage of this rule is that in the case of faster convergence of the emitter location algorithm (for small error triangles) to the fixed value (e.g. with an accuracy of 1 m), all other iterations of calculations are performed which do not have a significant impact on the estimated coordinates

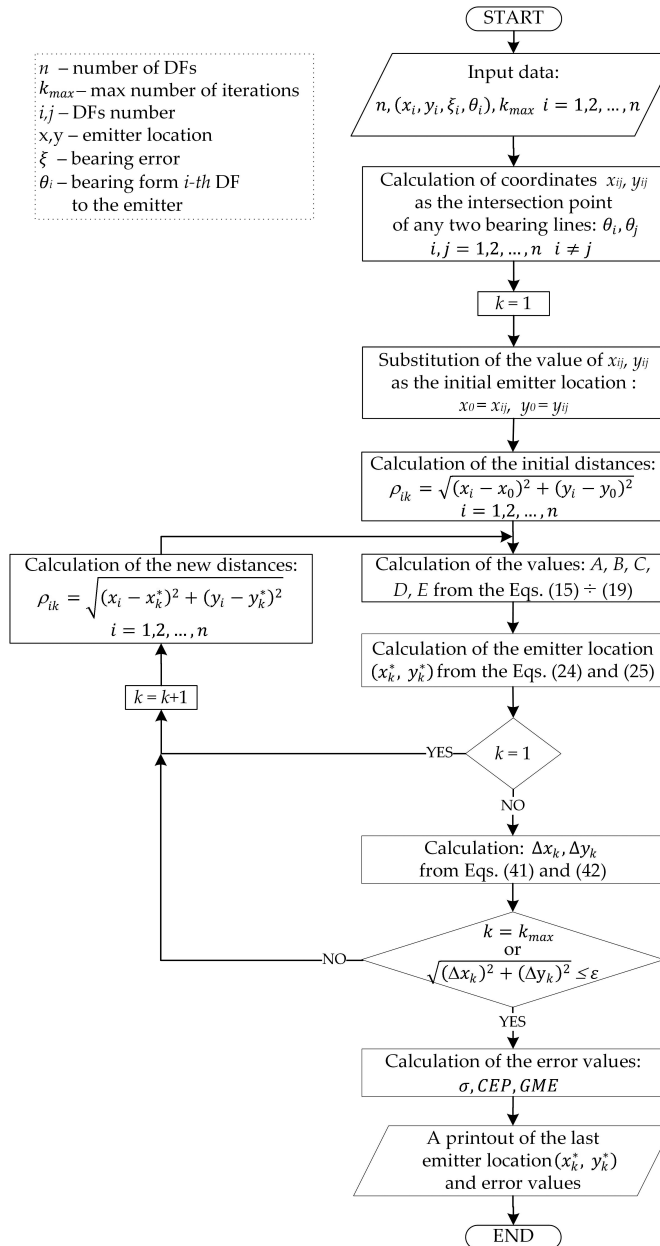


Fig. 5. Block diagram of the algorithm for calculating the emitter's location in the plane.

The number of performed iteration steps can be useful in evaluating some complex situations, e.g., with wrong leads (large error triangles) where the number of iterations can be large. The iteration process in the second rule is stopped when the changes of the coordinates $(\Delta x_k, \Delta y_k)$ of the emitter location in a given step k and in the previous step $k - 1$ are smaller than the given calculation accuracy error ε .

The quantities $\Delta x_k, \Delta y_k$ are calculated here as follows:

$$\Delta x_k = |x_k^* - x_{k-1}^*|, \quad \Delta y_k = |y_k^* - y_{k-1}^*|. \quad (36)$$

This method of stopping is selected when the user can specify numerical limits on the emitter location estimation errors. The process of estimating the emitter's location can be stopped here if the following relation is met:

$$\sqrt{(\Delta x_k)^2 + (\Delta y_k)^2} \leq \varepsilon. \quad (37)$$

The triangular method depends on iterative calculations of the estimated coordinates (x^*, y^*) for the emitter's location using (15)–(17) to calculate A, B, C, D, E. For solving these equations, knowledge about the distances from DF sensors' sites to the emitter's position is needed. In the first step of this iterative method, any distances can be taken for calculations, for example the point of intersection of two bearings. The distances from the DFs to the emitter's position are not calculated precisely at first. Therefore, they are more and more precise in the subsequent steps of the estimation. On the basis of a given number of bearing measurements for the same fixed emitter location a set of points was obtained, in which the detected emitter should be placed with a given probability.

4. Simulation experiment for determining the accuracy of the location system

In order to investigate the properties of the proposed modified method of calculating the emitter's location and to identify the possible errors in its location, a computer program in MATLAB was developed. The simulation tests were carried out for nine different variants of the DFs and emitter deployment in the given recognition area. The coordinates of the DFs for these tested variants are presented in Table 1.

Table 1. Variants of DFs deployment and their x, y coordinates [km] in the reconnaissance area.

Number of DFs	Name of deployment variant	Coordinates (x_i, y_i) of the DFs									
		DF ₁		DF ₂		DF ₃		DF ₄		DF ₅	
		x_1	y_1	x_2	y_2	x_3	y_3	x_4	y_4	x_5	y_5
3	C3_1*	0	0	25	0	50	0				
	C3_2		0		5		0				
	C3_3		5		0		5				
4	C4_1	0	0	15	0	35	0	50	0	50	
	C4_2		5		0		0		5		
	C4_3		10		0		0		10		
5	C5_1	0	0	12.5	0	25	0	37.5	0	50	
	C5_2		8		4		0		4		
	C5_3		12		4		0		4		

* C3_1 – denotes the variant 1 for three DFs

In the first stage, the properties of the algorithm itself and its convergence to the predetermined value (depending on the number of iterations) were examined. Because there are unknown distances from the emitter to the DFs in the final formulas (21) for calculating the emitter's

position, then in the zero step ($k = 0$) they are taken as the distances between the calculated intersection of the bearings from any two DFs. In the following iterations ($k = 1, 2, \dots$), the distances ρ_{ik} between the calculated emitter location (x^*, y^*) and locations of the DFs are already used.

The results of calculating the emitter's position in subsequent k iterations for different emitter locations (from the area of interest) are shown in Table 2.

Table 2. Algorithm convergence test (variant C3_1).

		The calculated location (x^*, y^*) in subsequent iterations k for the proposed algorithm						
Emitter location [km]	Iteration number k	0	1	2	3	4	5	6
$x = 10$		10.8411	10.3210	10.3196	10.3195	10.3195	10.3195	10.3195
$y = 15$		14.6049	15.0592	15.0582	15.0582	15.0582	15.0582	15.0582
$x = 20$		21.2325	20.5299	20.5225	20.5225	20.5225	20.5225	20.5225
$y = 40$		38.4768	10.2277	10.2341	40.2342	40.2342	40.2342	40.2342
$x = 25$		25.0106	25.0081	25.0079	25.0079	25.0079	25.0079	25.0079
$y = 5$		4.8744	5.0739	5.0740	5.0740	5.0740	5.0740	5.0740
$x = 25$		24.6983	24.9518	24.9501	24.9501	24.9501	24.9501	24.9501
$y = 35$		36.2994	35.5362	35.5387	35.5386	35.5386	35.5386	35.5386
$x = 35$		35.4815	35.1317	35.1283	35.1282	35.1282	35.1282	35.1282
$y = 50$		48.3006	51.0559	51.0891	51.0895	51.0895	51.0895	51.0895
$x = 45$		45.1181	45.0853	45.0853	45.0853	45.0853	45.0853	45.0853
$y = 10$		9.8742	9.9515	9.9516	9.9516	9.9516	9.9516	9.9516

Based on the obtained calculation results, it can be seen that the calculated position of the emitter is based on the given bearings of this emitter with the RMS error equal to 1° for all DFs and converges to the value determined with an accuracy $\varepsilon \leq 0.1$ m after 3–4 iterations (Table 2). Such results are achieved despite the fact that in step $k = 0$ the point of intersection of bearings from two DFs was taken as the starting point of the emitter's position, which differs significantly from the end position.

The results presented in the table above also show that the emitter's location calculated only based on single bearings may differ significantly from the real emitter location. For the fifth variant of the emitter's position ($x = 35$, $y = 50$) [km], the location differs even by more than 1 km for the y -coordinate.

The precise estimation of emitter location can be performed if a sufficient number of bearings is available.

In connection with the considerations above, it can be concluded that the use of such a modification (introducing iteration of the algorithm) improves the accuracy of the object's location in the triangulation method.

The estimated area of calculated errors CEP , GME , elliptical, and triangle are shown in Fig. 6 for 4 different configurations of the emitter and the DFs. For every variant of the deployment of

the DFs and the emitter, 100 bearings were generated from the Gaussian normal distribution with the standard deviation equalling 1° . The calculated emitter locations are marked in green.

The evaluation of emitter location accuracy based on (21) was performed using a simulation program, in which the real emitter position (x, y) was assumed as known, and for this location a set of N bearings was generated for every DF from normal distribution $\text{Normal}(\theta_i^t, \xi_{\theta_i})$ where θ_i^t denotes a theoretical bearing calculated for the i -th DF placed in the point (x_i, y_i) and ξ_{θ_i} is the root mean square (RMS) error of bearings for the i -th DF. To determine the precise emitter location, a minimal number of generated bearings at the same electromagnetic source is needed.

Assuming the Gaussian normal distribution of bearing errors [1, p. 108], the best centre is grouped in a normal elliptical error distribution, and it is convenient to visualize this by drawing an ellipse so that 50% of the location fixes are inside the ellipse and 50% are outside the ellipse [1, pp. 107–108], [13, pp. 173–174].

Figs. 6, 7 show that the best mapping of 50% of the emitter location error area is for the elliptical error. It is especially pronounced when the emitter is closer to the end positions of the DFs. By comparing the CEP and GME errors, it can be stated that for all tested DFs and settings, the GME error area is larger.

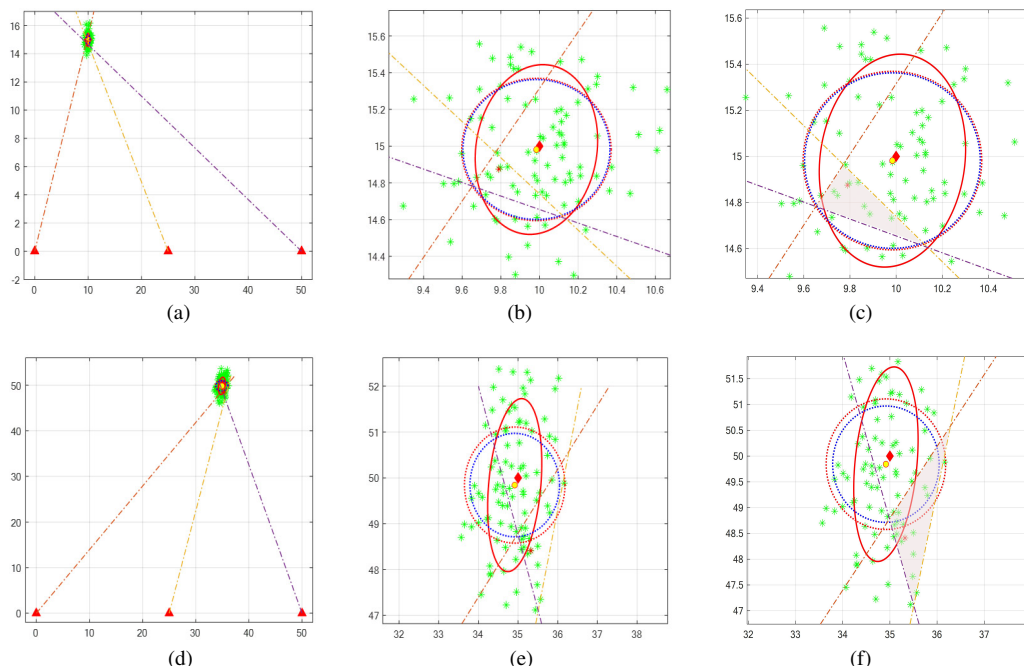


Fig. 6. Area of emitter location errors (in OXY plane [km]) for different deployment of three DFs: (a–c) emitter in tested point $(10, 15)$ [km]; (d–f) emitter in tested point $(35, 50)$ [km].

The simulation experiment for the proposed algorithm was performed for:

- a different number n of DFs;
- different mutual deployment of DFs and the emitter in the reconnaissance area;
- different RMS of bearings: $\xi_1, \xi_2, \dots, \xi_n$ for DFs;
- different number of N bearings made from every DF in the known emitter location.

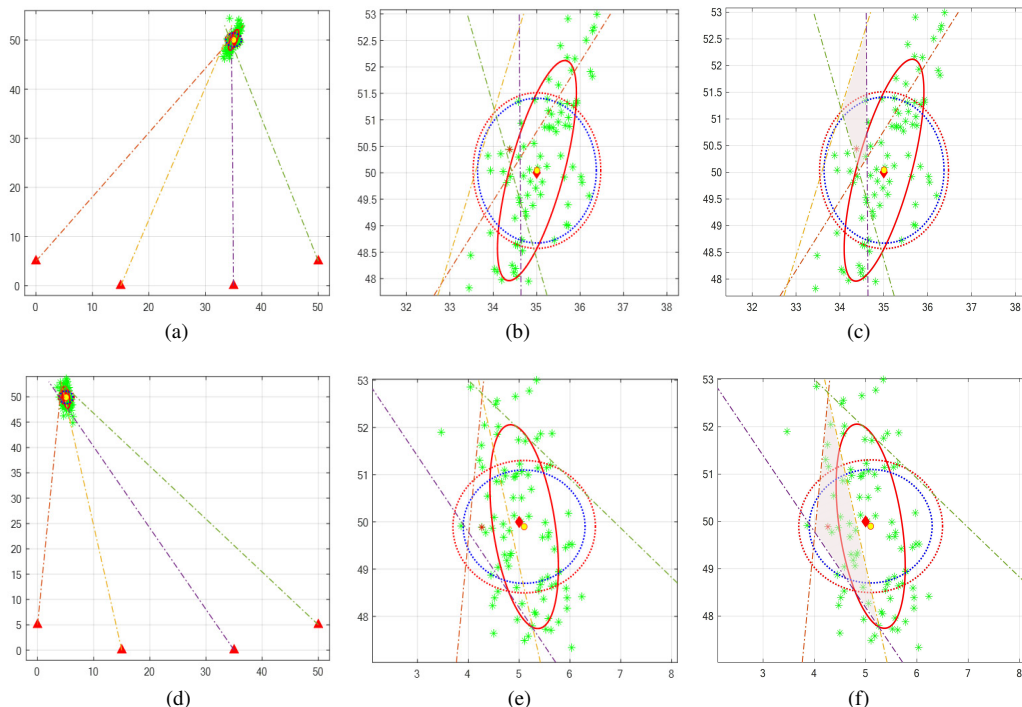


Fig. 7. Area of emitter location errors (in OXY plane [km]) for different deployment of four DFs: (a–c) emitter in tested point (35, 50) [km]; (d–f) emitter in tested point (5, 50) [km].

The symbols used in Fig. 6 and 7 mean:

	Estimated emitter location		Analyzed emitter		Bearing from DF ₁
	Direction finder location		CEP error		Bearing from DF ₂
	Emitter location		GME error		Bearing from DF ₃
	Mean value of emitter location				Bearing from DF ₄

The results of the simulation for different variants of deployment DFs and the emitter are depicted in Figs. 8 to 13 and in Table 3.

Figure 8 shows the results of simulation of the emitter's location at tested point (15, 45) [km] and the values of the emitter location errors, calculated based on 100 randomly drawn bearings from the normal distribution and three different RMS errors. On the basis of such a large series of measurements, it can be concluded that the calculated position of the emitter can differ for the test position from several hundred meters up to 2.7 kilometre. A twofold increase in RMS errors also causes an approximately twofold increase in the analysed errors (σ , CEP and GME) in estimating the emitter's position (Fig. 8a). The averaged position of the emitter (Fig. 8b) based on the 100 bearings generated is practically the same regardless of the different RMS errors ($\xi = 0.5^\circ$, $\xi = 1^\circ$ and $\xi = 2^\circ$) of the DFs. This means that with a large number of bearings measured at the same emission source, its position can be calculated with an accuracy of several kilometres, even with a relatively large RMS error of the DFs (Fig. 8b).

Figure 9 shows the RMS errors of the emitter's location obtained from the simulation for 3 and 4 DFs based on 100 generated bearings in the three-dimensional space in the set reconnaissance

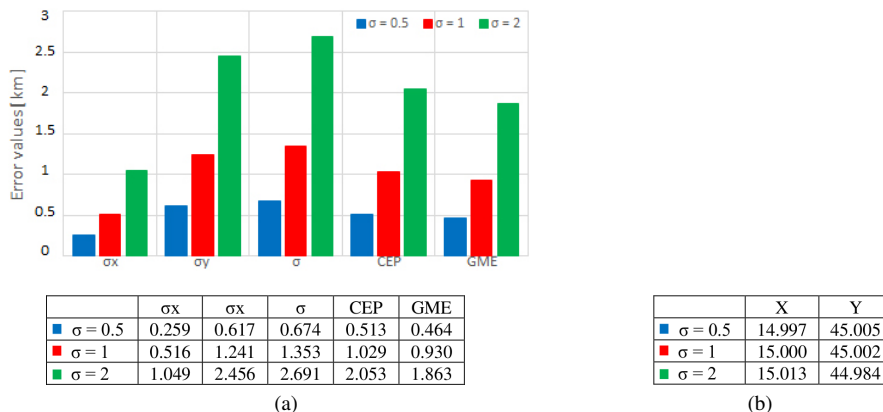


Fig. 8. Simulation results for emitter location (x, y) and errors values ($\sigma_x, \sigma_y, \sigma, CEP$ and GME) in tested point (15, 45) [km] calculated for variant C3_1 based on 100 generated values of the bearings and 3 measurement accuracies of DFs ($\xi = 0.5^\circ$, $\xi = 1^\circ$ and $\xi = 2^\circ$): (a) averaged values of errors and (b) averaged values of emitter location.

area with 1 km step changes of the emitter's location. The values of RMS errors are presented using the appropriate colour gradation marked in the right-hand bar of the graphs. The greatest error in determining the emitter's location (e.g. about 2.2 km in Fig. 9b and about 4.4 km in Fig. 9f occurs at the extreme points and the farthest from the centre of the DF position. In the variant with 4 DFs, this error is about two times smaller in the area near the position of DF₁ and DF₂.

Figure 10 shows the average of three different emitter location estimation errors (σ , CEP , and GME) calculated on the basis of N ($N = 10, 20, 30, 40$, and 50) randomized bearings from the normal distribution for every DF. Increasing the number of bearings from 10 to 50 does not have too much influence on the values of these errors, which increased by a dozen or so (several dozen meters for the emitter located at point (40, 40) [km]).

The averaged position of the emitter for the test point (40, 40) shows that the number of bearings taken for the calculation ($N = 10, 20, 30, 40, 50$) does not affect the accuracy of the location of the emitter, while the differences between the minimum and maximum values can exceed even the value of 1 km, (Fig. 10b). This means that in a real reconnaissance system, it is enough to make about 10 measurements of bearings of a given emission source in order to obtain the precise location of the emitter.

In order to verify the correctness of the presented maximum likelihood method for calculating the emitter's location and the associated location errors, 100 bearings were generated from every DF to the emitter's position at testing point (10, 15) [km]. The results of the simulation tests are shown in Fig. 11 for all variants of the DFs' settings, (Table 1). The averaged coordinates of the emitter location calculated in this way differ from the known emitter location by only a few meters.

The comparison of estimation errors for the emitter's position in tested point (10, 15) [km] for all variants of DFs deployment is shown in Fig. 11.

Based on the obtained simulation results, it can be concluded that the smallest errors were obtained when the side DFs were moved forward, both for 3, 4, and 5 DFs (variants C3_3, C4_3, and C5_3). On the right side of the estimation errors in Fig. 11, the average emitter positions (X, Y) and the minimum and maximum values (X_{\min}, X_{\max}), (Y_{\min}, Y_{\max}) are given, obtained on the basis of 100 calculated emitter locations according to (21).

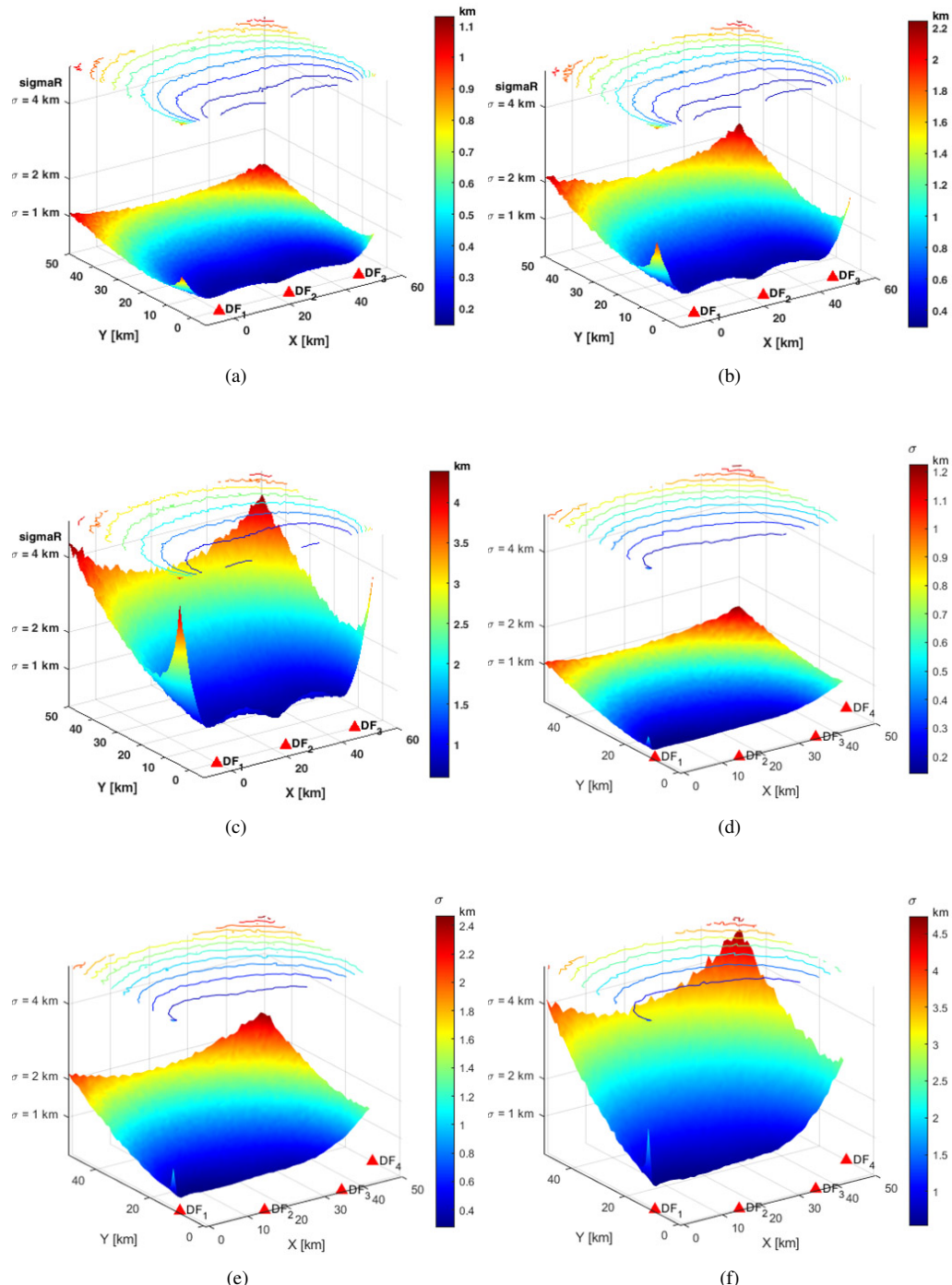


Fig. 9. Distribution of RMS errors of estimated emitter location along the x and y axes, calculated with 1 km step in the analysed reconnaissance area and averaged based on 100 generated bearings with the same RMS errors for every DF:
 (a) $\xi_1 = 0.5^\circ$; (b) $\xi_2 = 1^\circ$; (c) $\xi_3 = 2^\circ$ for variant C3_1, area $(x \in (-10, 60) \text{ km}, y \in (-4, 50) \text{ km})$, and (d) $\xi_1 = 0.5^\circ$; (e) $\xi_2 = 1^\circ$; (f) $\xi_3 = 2^\circ$ for variant C4_3, area $(x \in (-1, 50) \text{ km}, y \in (11, 50) \text{ km})$.

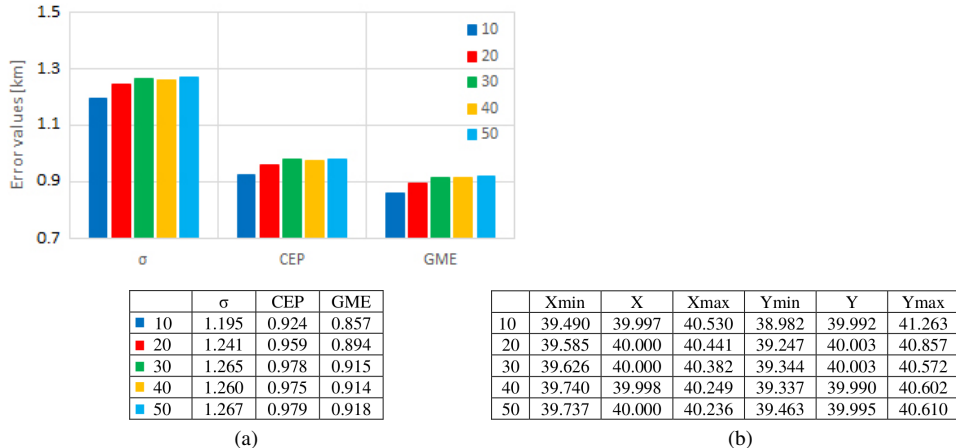


Fig. 10. Average values of errors in estimating the emitter position in tested point (40, 40) [km] depending on the number of bearings N ($N = 10, 20, 30, 40$, and 50) based on 100 simulated realizations for the variant C3_1, RMS for every DF equal to 1° .

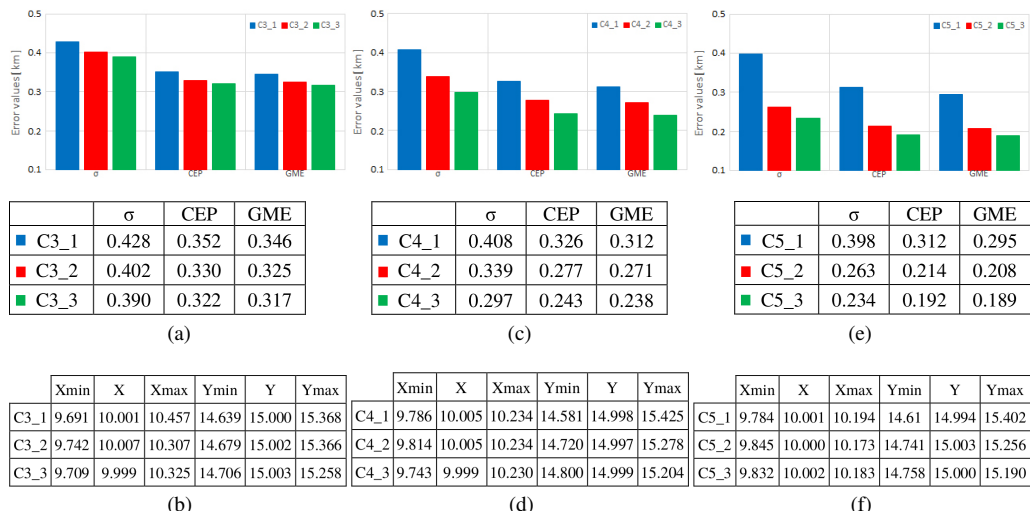


Fig. 11. Estimation of emitter location errors (σ , CEP and GME) located in tested point (10, 15) [km] for all configurations of DFs deployment (100 generated bearings realizations, accuracy of bearing error measurement $\xi = 1^\circ$: (a–b) variants for 3 DFs; (c–d) variants for 4 DFs; (e–f) variants for 5 DFs).

Similarly, a comparison of estimation errors for the emitter's position in tested point (45, 50) [km] (significant distances from the DFs) for all the examined variants of DFs deployment is shown in Fig. 12. Also in this case, the smallest errors were obtained when the side DFs were moved forward, for 3, 4, and 5 DFs (variants C3_3, C4_3, and C5_3).

The high accuracy of calculating the position of the emitter on the basis of a large number of bearings ($N = 100$) is confirmed by the results of calculations presented in Figs. 11–13 for 3, 4 and 5 DFs and 2 test points (10, 15) and (45, 50). The calculation of the averaged emitter position is also not significantly influenced by the addition of a 4th and 5th DF, but the errors (σ , CEP

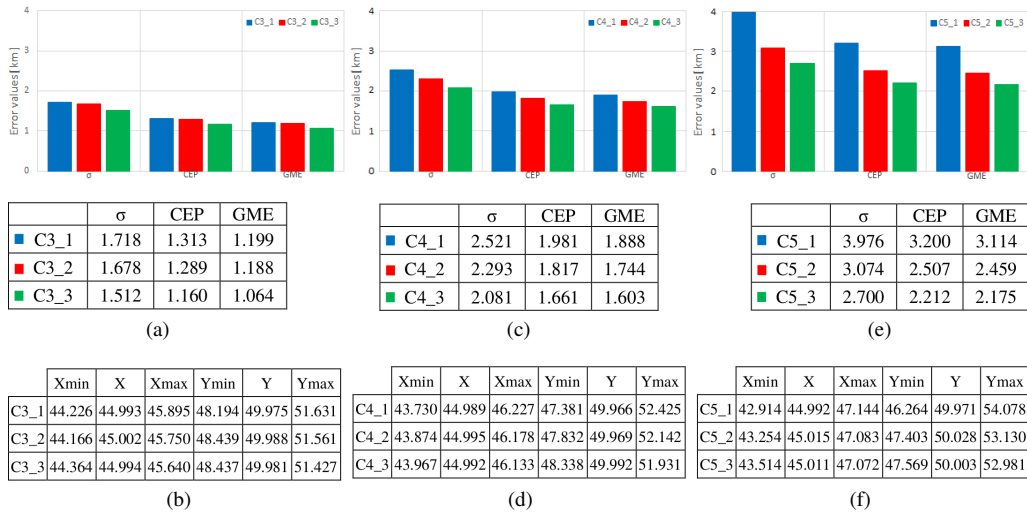


Fig. 12. Estimation of emitter location errors (σ , CEP and GME) located in tested point (45, 50) [km] for 9 configurations of DFs deployment (100 generated bearings realizations, accuracy of the bearings error measurement $\xi = 1^\circ$: (a–b) variants for 3 DFs; (c–d) variants for 4 DFs; (e–f) variants for 5 DFs.

and GME) increase. The difference between the test value (x , y) and the minimum or maximum value in the (x_{\min} , x_{\max}) or (y_{\min} , y_{\max}) for single bearings taken for the calculations can even reach 3 km (Figs. 11–12).

Table 3. Improvement of accuracy of emitter location depending on DF configuration.

Emitter location test point(10, 15)	σ							
	3 DF				4 DF			
	C3_1	0.428	C4_1	0.408	C5_1	0.398	C5_2	0.263
C3_2	0.402	6%	C4_2	0.339	17%	C5_3	0.234	41%
C3_3	0.391	9%	C4_3	0.297	27%	C5_1	3.976	23%

Emitter location test point (45, 50)	σ							
	C3_1	1.718		C4_1	2.521		C5_1	3.976
	C3_2	1.678	2%	C4_2	2.293	9%	C5_2	3.074
	C3_3	1.512	12%	C4_3	2.081	17%	C5_3	2.700

On the basis of the simulation experiment carried out, it can be seen that in all the tested points for 3, 4 and 5 DFs, the forward movement of the DFs deployed from the left and right side of the main DF reduces the errors (σ) from a few to over 40%, (Table 3).

Figure. 13 shows a comparison of emitter location errors (σ , CEP, and GME) for 9 variants of DF deployment and two different emitter positions: (10, 15) [km] and (45, 50) [km]. The farther the emitter is located from the DFs, the greater these errors are.

Depending on the position of the emitter in relation to the DFs, these averaged errors on the basis of many bearings can range from several hundred meters (Fig. 13a) to several kilometres (Fig. 13b).

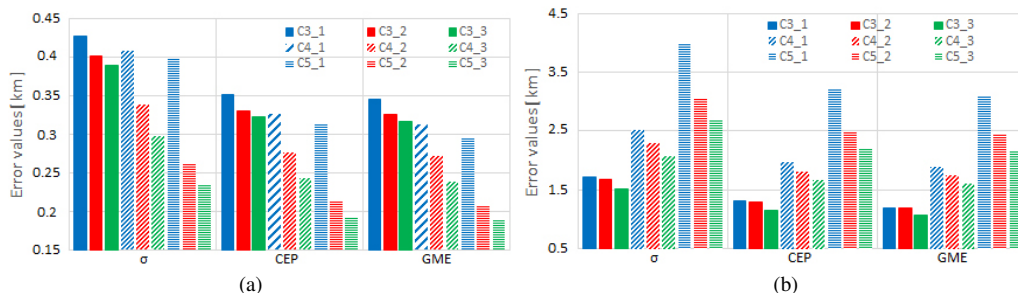


Fig. 13. Average values of errors of emitter location for 9 variants of DF deployment (100 generated bearings realizations, accuracy of bearings error measurement $\xi = 1^\circ$: (a) emitter located in tested point (10, 15) [km]; (b) emitter located in tested point (45, 50) [km].

5. Conclusions

In this paper, the effect of different errors on estimation of emitter location was presented. A theoretical expression for emitter location uncertainty in terms of errors for different configurations of the emitter and DFs deployment was derived and used to calculate error ellipse parameters for the triangulation method.

The following factors should be taken into consideration in the process of performing the measurements of bearings: the choice of the method of location using an appropriate measurement technique, determining the number of DFs, their deployment in the reconnaissance area, and the number of bearings taken to calculate the estimated emitter location.

The features of the proposed method were examined using the simulation data for the known emitter's location and given parameters of the DF system. Numerical calculations show in which way the area of uncertainty of the emitter's location changes. These results can be used to select such a deployment of direction finders in a given reconnaissance area which will ensure a minimum error in determining the coordinates of the unknown emitter location. The higher the number of bearings, the better the accuracy of calculating the emitter's location, in spite of relatively high bearing errors for every DF.

The iterative algorithm of calculating the emitter's position presented in this article – a way of selecting the initial distance between the unknown position of the emitter and the number of bearings taken to calculation – can be directly used in electronic reconnaissance and warfare systems. The simulation results obtained for a large sample of generated bearings for three, four, and five DFs in different variants of their deployment confirmed its high accuracy.

The obtained results are promising and make it possible to use them for planning the deployment of DFs in a real electromagnetic environment.

In the next stage of the research, the optimal deployment of DFs should be determined in order to minimize the emitter's location error in the entire recognition area, also taking into consideration their technical properties.

Acknowledgements

This work was financed/co-financed by the Military University of Technology under Research Project UGB 22-856.

References

- [1] Willey, R. G. (1985). *Electronic Intelligence: The Interception of Radar Signals*. Artech House.
- [2] Oshman, Y., & Davidson, P. (1999). Optimization of observer trajectories for bearings-only target localization. *IEEE Transactions on Aerospace and Electronic Systems*, 35(3), 892–902. <https://doi.org/10.1109/7.784059>
- [3] Tehrani, M. A., Laurin, J. J., & Savaria, Y. (2016). Multiple targets direction-of-arrival estimation in frequency scanning array antennas. *IET Radar, Sonar & Navigation*, 10(3), 624–631. <https://doi.org/10.1049/iet-rsn.2015.0401>
- [4] Rutkowski, A., & Kawalec, A. (2020). Some of Problems of Direction Finding of Ground-Based Radars Using Monopulse Location System Installed on Unmanned Aerial Vehicle. *Sensors*, 20(18), 5186. <https://doi.org/10.3390/s20185186>
- [5] Wang, Y., Jie, H., & Cheng, L. (2019). A Fusion Localization Method based on a Robust Extended Kalman Filter and Track-Quality for Wireless Sensor Networks. *Sensors*, 19(16), 3638. <https://doi.org/10.3390/s19173638>
- [6] Chow, T. L. (2001). Passive emitter location using digital terrain data [Doctoral dissertation, Binghamton University State University of New York].
- [7] Poisel, R. A. (2012). *Electronic Warfare Target Location Methods* (2nd. ed.). Artech House.
- [8] Willey, R. G. (2006). *ELINT. The Interception and Analysis of Radar Signals*. Horizon House Publications.
- [9] Chan, Y. T., & Ho, K. C. (1994). A simple and efficient estimator for hyperbolic location. *IEEE Transactions on Signal Processing*, 42(8), 1905–1915. <https://doi.org/10.1109/78.301830>
- [10] Bugaj, J., & Górný, K. (2019, March). Analysis of estimation algorithms for electromagnetic source localization. In *XII Conference on Reconnaissance and Electronic Warfare Systems* (Vol. 11055, p. 110550W). International Society for Optics and Photonics. <https://doi.org/10.1117/12.2524927>
- [11] O'Connor, A., Setlur, P., & Devroye, N. (2015). Single-sensor RF emitter localization based on multipath exploitation. *IEEE Transactions on Aerospace and Electronic Systems*, 51(3), 1635–1651. <https://doi.org/10.1109/TAES.2015.120807>
- [12] Adamy, D. L. (2001). *EW 101. A First Course in Electronic Warfare*. Artech House.
- [13] Adamy, D. L. (2004). *EW 102. A Second Course in Electronic Warfare*. Horizon House Publications.
- [14] Becker, K. (1992). An efficient method of passive emitter location. *IEEE Transactions on Aerospace and Electronic Systems*, 28(4), 1091–1104. <https://doi.org/10.1109/7.165371>
- [15] Foy, W. H. (1976). Position-location solutions by Taylor-series estimation. *IEEE Transactions on Aerospace and Electronic Systems*, AES-12(2), 187–194. <https://doi.org/10.1109/TAES.1976.308294>
- [16] Mangel, M. (1981). Three Bearing Method for Passive Triangulation in Systems with Unknown Deterministic Biases. *IEEE Transactions on Aerospace and Electronic Systems*, AES-17(6), 814–819. <https://doi.org/10.1109/TAES.1981.309133>
- [17] Adamy, D. L. (2005). Emitter Location: Reporting Location Accuracy. *The Journal of Electronic Defense*, (7).
- [18] Kelner, J. M., & Ziolkowski, C. (2020). Effectiveness of Mobile Emitter Location by Cooperative Swarm of Unmanned Aerial Vehicles in Various Environmental Conditions. *Sensors*, 20(9), 2575. <https://doi.org/10.3390/s20092575>
- [19] Mahapatra, P. R. (1980). Emitter location independent of systematic errors in direction finders. *IEEE Transactions on Aerospace and Electronic Systems*, AES-16(6), 851–855. <https://doi.org/10.1109/TAES.1980.309009>

- [20] Matuszewski, J., & Dikta, A. (2017, April). Emitter location errors in electronic recognition system. In *XI Conference on Reconnaissance and Electronic Warfare Systems* (Vol. 10418, p. 104180C). International Society for Optics and Photonics. <https://doi.org/10.1117/12.2269295>
- [21] Stansfield, R. G. (1947). Statistical theory of DF fixing. *Journal of the Institution of Electrical Engineers-Part IIIA: Radiocommunication*, 94(14), 762–770. <https://doi.org/10.1049/ji-3a-2.1947.0096>
- [22] Vakin, S. A., Shustov, L. N., Dunwell, R. H. (2001). *Fundamentals of Electronic Warfare*. Artech House.
- [23] Bature, U. I., Tahir, N. M., Yakub, N. A., & Baba, M. A. (2020). Multi-baseline Emitter Location System: A Correlative Interferometer Approach. *Nigerian Journal of Engineering*, 27(2), 92–98.
- [24] Becker, K. (1992). An efficient method of passive emitter location. *IEEE Transactions on Aerospace and Electronic Systems*, 28(4), 1091–1104. <https://doi.org/10.1109/7.165371>
- [25] Tian, B., Huang, H., & Li, Y. (2009, September). Direction of arrival estimation using nonlinear function of sum and difference beam. In *2009 IEEE Youth Conference on Information, Computing and Telecommunication* (pp. 311–314). IEEE. <https://doi.org/10.1109/YCICT.2009.5382360>
- [26] Ghilani, C. D., & Wolf, P. R. (2007). *Adjustment Computations: Spatial Data Analysis* (4th ed.). John Wiley & Sons, Inc. <https://doi.org/10.1002/9780470121498>
- [27] Gavish, M., & Weiss, A. J. (1992). Performance analysis of bearing-only target location algorithms. *IEEE Transactions on Aerospace and Electronic Systems*, 28(3), 817–828. <https://doi.org/10.1109/7.256302>
- [28] He, Y., Behnad, A., & Wang, X. (2015). Accuracy analysis of the two-reference-node angle-of-arrival localization system. *IEEE Wireless Communications Letters*, 4(3), 329–332. <https://doi.org/10.1109/LWC.2015.2415788>
- [29] Kukes, I. S., Starik, M. Ye. (1964). *Principles of Radio Direction Finding*. Soviet Radio Publishing House. (in Russian)
- [30] Paradowski, L. R. (1998, May). Microwave emitter position location: present and future. In *12th International Conference on Microwaves and Radar. MIKON-98. Conference Proceedings* (IEEE Cat. No. 98EX195) (pp. 97–116). IEEE. <https://doi.org/10.1109/MIKON.1998.738464>
- [31] Paradowski, L. R. (1997). Uncertainty ellipses and their application to interval estimation of emitter position. *IEEE Transactions on Aerospace and Electronic Systems*, 33(1), 126–133. <https://doi.org/10.1109/7.570715>
- [32] Rui, L., & Ho, K. C. (2014). Elliptic localization: Performance study and optimum receiver placement. *IEEE Transactions on Signal Processing*, 62(18), 4673–4688. <https://doi.org/10.1109/TSP.2014.2338835>
- [33] Shirman Ya. D. (Eds.). (1970). *Theoretical fundamentals of radiolocation*. Sovetskoe Radio. (in Russian)
- [34] Tondwalkar, A. V., & Vinayakray-Jani, P. (2015, December). Terrestrial localization by using angle of arrival measurements in wireless sensor network. In *2015 International Conference on Computational Intelligence and Communication Networks (CICN)* (pp. 188–191). IEEE. <https://doi.org/10.1109/CICN.2015.44>
- [35] Wang, Z., Luo, J. A., & Zhang, X. P. (2012). A novel location-penalized maximum likelihood estimator for bearing-only target localization. *IEEE Transactions on Signal Processing*, 60(12), 6166–6181. <https://doi.org/10.1109/TSP.2012.2218809>
- [36] Ziolkowski, C., & Kelner, J. M. (2015). The influence of propagation environment on the accuracy of emission source bearing. *Metrology and Measurement Systems*, 22(4), 591–600.



Jan Matuszewski received the M.Sc. degree in Cybernetics and the Ph.D. degree in Telecommunication from the Military University of Technology (MUT), Poland, in 1972 and 1984, respectively. He has worked at the MUT since 1972. He has published over 170 research papers in the national and international journals, and conference proceedings. He has received several awards for his contribution to the projects in ESM/ELINT stations from his University Rector and the Ministry of

National Defence. His research activity focuses on electronic warfare, emitter localization and recognition, radar jamming, neural networks and artificial intelligence.



Tomasz Kraszewski received the M.Sc. degree in Electronics and Telecommunication from the Military University of Technology (MUT) in 1999 and he has worked at the MUT since then. He has published over 40 research papers in the field of localization and navigation for national and international journals, and conference proceedings. His main research interests are design and improvement of nonlinear filtering in such applications as location, navigation and medical systems.